Journal of Catalysis 269 (2010) 411–420

Contents lists available at ScienceDirect

Journal of Catalysis

journal homepage: www.elsevier.com/locate/jcat

Towards understanding the bifunctional hydrodeoxygenation and aqueous phase reforming of glycerol

A. Wawrzetz, B. Peng, A. Hrabar, A. Jentys, A.A. Lemonidou [1], J.A. Lercher *

Department Chemie, Technische Universität München, Lichtenbergstraße 4, 85747 Garching, Germany

ARTICLE INFO

Article history:
Received 21 August 2009
Revised 19 November 2009
Accepted 26 November 2009
Available online 4 January 2010

Keywords:
Hydrodeoxygenation of alcohols
Aqueous phase reforming
Glycerol
ATR-IR spectroscopy

ABSTRACT

Kinetically coupled reactions of glycerol in water over bifunctional Pt/Al_2O_3 catalysts are explored as a function of the Pt particle size and the reaction conditions. Detailed analysis of the reaction network shows that "reforming" and hydrodeoxygenation require the presence of a bifunctional catalyst, i.e., the presence of an acid–base and a metal function. The initial reaction steps are identified to be dehydrogenation and dehydration. The dehydrogenation of hydroxyl groups at primary carbon atoms is followed by decarbonylation and subsequent water gas shift or by disproportionation to the acid (and the alcohol) followed by decarboxylation. Hydrogenolysis of the C–O and C–C bonds in the alcohols does not occur under the present reaction conditions. Larger Pt particles favor hydrodeoxygenation over complete deconstruction to hydrogen and CO_2.

1. Introduction

Routes for hydrogen and chemicals production from renewable sources such as biomass pyrolysis oil, bio-ethanol, and glycerol [1–11] are currently of high interest, because biogenic resources provide an interesting niche route to valuable energy carriers. Among these feedstocks glycerol is still an attractive resource due to its ample availability as a by-product formed in bio-diesel production and a model compound allowing not only to explore the conversion to H_2 and CO_2, but also details of the chemical transformations in multiple alcohols.

Reforming of glycerol in the aqueous phase (APR) is carried out at relatively low temperatures (423–523 K) and elevated pressures (15–60 bar) [7–14]. This avoids the evaporation of water and reduces CO formation, because of the more favorable equilibrium of the water gas shift reaction at the lower temperatures [15]. However, in addition to reforming and water gas shift, reactions such as hydrogenation of carbon monoxide and hydrogenation and hydrogenolysis of glycerol to diols have been reported to occur. The overall reaction pathways of an aqueous phase reforming of biomass-derived alcohols have been discussed excellently by Dumesic et al. [7–14] and Davis et al. [16,17].

In general, the catalysts active for an aqueous phase reforming are claimed to have a high catalytic activity for the water gas shift reaction and a sufficiently high catalytic activity for C–C bond cleavage. Catalysts active for CO hydrogenation lead to a lower hydrogen selectivity and to the appearance of light alkanes. Acidic supports in combination with a metal favor dehydration/hydrogenation reactions consuming hydrogen [18]. Among the different noble and base metals, Pt was the most selective catalyst for hydrogen formation [18] and among the different supports investigated [19], Pt supported on Al_2O_3 showed the highest hydrogen selectivity (>90%). It was noted, however, that γ-Al_2O_3 is not stable under the typical reaction conditions of the aqueous phase reforming reaction [20]. The selectivity to H_2 is said to increase with increasing Pt particle size because of the enhanced rate of C–C bond cleavage on Pt ensembles on low index metal surfaces [21]. In contrast, we showed recently that the cleavage of C–C and C–O bonds did not occur with cyclic secondary alcohols under nearly identical reaction conditions [22].

In order to explore to what extent C–C and C–O bond cleavage play a role in the aqueous phase conversion of polyols, the catalytic conversion of glycerol in water over Pt/Al_2O_3 was explored under reaction conditions favoring the formation of intermediate chemicals. Special emphasis was given to the various pathways leading to hydrogen and carbon oxides as well as to hydrodeoxygenation utilizing hydrogen generated from converting a fraction of glycerol.

2. Experimental section

2.1. Catalysts preparation

Pt supported on γ-Al_2O_3 with loadings of 1, 3, and 5 wt.% were prepared by incipient wetness impregnation. Platinum (II)-ammonium nitrate (Strem chemicals) was used as a precursor. The

* Corresponding author. Fax: +49 89 289 135 44.
E-mail address: johannes.lercher@ch.tum.de (J.A. Lercher).
[1] Permanent address: Department of Chemical Engineering, Aristotle University Thessaloniki University City Thessaloniki, 54124 Greece.

0021-9517/$ - see front matter © 2009 Elsevier Inc. All rights reserved.
doi:10.1016/j.jcat.2009.11.027

support was γ-Al_2O_3 (Aeroxide Alu C-Degussa) with a surface area of 150 m^2/g. After impregnation of the support with the aqueous precursor solution, the catalysts were dried in air at 393 K for 12 h and calcined in synthetic air for 2 h at 573 K. Prior to reaction and characterization, the catalysts were reduced in H_2 at 623 K for 2 h. It should be noted that during the catalytic reaction γ-Al_2O_3 was converted to pseudo boehmite, but was not dissolved or caused blocking or deactivation of the catalyst. Pt black with a specific surface area of 25 m^2/g was obtained from Sigma–Aldrich.

2.2. Catalyst characterization

2.2.1. Atomic absorption spectroscopy (AAS)

The concentration of the metal was determined by atomic absorption spectroscopy using a UNICAM 939 AA-Spectrometer. Typically, 20–40 mg of the sample was dissolved in a mixture of 0.5 ml of hydrofluoric acid (48%) and 0.1 ml of nitro-hydrochloric acid at the boiling point of the mixture (about 383 K).

2.2.2. Hydrogen and nitrogen sorption

The fraction of accessible Pt atoms was determined by H_2 chemisorption using a Sorptomatic 1990 Series instrument. Approximately 1 g of catalyst was reduced in H_2 at 588 K for 1 h, followed by outgassing in vacuum at 308 K for 4 h. The sorption isotherms were measured at 308 K. The amount of chemisorbed hydrogen was obtained after removing physisorbed hydrogen from the sample by evacuation at 308 K for 2 h. The metal dispersion was determined by assuming H/Pt ratio of 1 [23]. The particle sizes of Pt were calculated by the relationship between dispersion and crystallite size [24] assuming spherical particles.

The BET surface area and pore size distribution were determined by N_2 adsorption–desorption at 77 K using a Sorptomatic 1990 Series instrument after the activation of the sample in vacuum at 573 K for 2 h.

2.2.3. Temperature-programed desorption (TPD)

Temperature-programed desorption of ammonia and carbon dioxide was performed under flow conditions. The catalysts were activated in helium at 623 K for 1 h using a heating rate of 5 K/min from room temperature to 623 K. Ammonia or carbon dioxide was adsorbed by adding 10 vol.% to the He carrier gas (total flow 30 ml/min) at 423 K or 308 K, respectively. The sample was purged with He for 2 h in order to remove physisorbed molecules. For TPD, the sample was heated in He at a rate of 10 K/min from 373 K to 1033 K for ammonia desorption and from 308 K to 673 K for carbon dioxide desorption. The species desorbing were monitored by mass spectrometry (Balzers QME 200). For quantification a standard with known acid site concentration (HZSM-5 with Si/Al = 45) was used. The response of the CO_2 signal was calibrated using the decomposition of $NaHCO_3$.

2.3. Kinetic measurements

The reaction system used for testing the catalyst performance is schematically shown in Fig. 1. The stainless steel tubular reactor (1/4 inch o.d.) was loaded with 50–160 mg catalyst with a particle size between 300 and 500 μm. After the reduction of the catalysts in H_2 at 623 K for 2 h, the system was purged and pressurized with nitrogen before starting the reaction. A liquid solution of glycerol ($\geqslant$99.5% purity, Aldrich) in deionized water was introduced in an up-flow configuration with a HPLC pump. The liquid and gaseous products leaving the reactor were cooled in a heat exchanger to liquefy condensable vapors. The effluent was mixed with nitrogen and the two phases were separated after the 16-port sampling valve in sixteen vials.

The liquid samples were analyzed in a gas chromatograph equipped with FID/MS detector and CP-Wax 57 CB column. To ensure the detection of all carbon containing species in the liquid products, the liquid samples were additionally analyzed by elemental analysis (Elemental Vario EL). Gaseous products were analyzed on line by a gas chromatograph with TCD and two capillary columns (MS-5S and Para Plot Q).

The influences of the metal particle size and the pressure (26–45 bar) were studied using a 20 wt.% glycerol solution (H_2O/C = 6.8) at 498 K. The effect of the glycerol concentration was investigated between 10 and 30 wt.% at 498 K and 29 bar. The conversion levels were kept in the same range (7–10%) for these measurements by varying the WHSV in order to allow a differential rate analysis. Furthermore, a series of experiments was conducted at 498 K and 29 bar by varying the weight hourly space velocity (WHSV) between 0.45 and 22.70 h^{-1} with a 30 wt.% glycerol solution (molar ratio of H_2O/C = 4) to attain high glycerol conversion

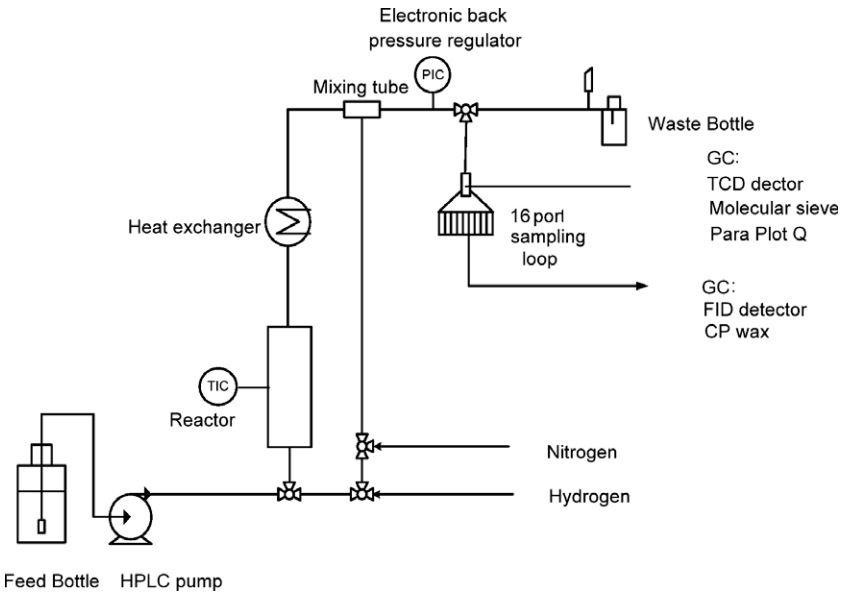

Fig. 1. Scheme of the reactor used for kinetic experiments.

levels. The reaction with hydroxyacetone being the intermediate with the highest concentration present in the aqueous phase was performed at a concentration of 10 wt.% with a space velocity in the range of 0.23–24.3 h^{-1}. Under the reported conditions all catalysts were stable. Slight initial deactivation was observed. The carbon balance was within 5% for all experiments. The carbon product selectivities were calculated by:

$$\text{Carbon selectivity} = \frac{\text{product formed } \left(\frac{\text{mmol}}{\text{min}}\right) \cdot \text{number of carbon atoms}}{\text{gylcerol feed } \left(\frac{\text{mmol}}{\text{min}}\right) \cdot \text{conversion} \cdot 3}$$

Selected experiments with 1-propanol, 2-propanol as well as with glycerol were conducted in a 300-ml batch autoclave. The reactants and the catalyst loaded in a closed glass vial were charged into the reactor. When the required temperature and pressure were reached, the reaction was started after breaking the glass vial by stirring. Blind tests showed that the thermal conversion under these conditions was negligible. The vapor phase was analyzed online by gas chromatography with a TCD and two capillary columns (MS-5A and HP-Plot Q). Liquid samples were manually collected during the run and analyzed in a gas chromatograph equipped with a FID and a CP-Wax 57CB column. The standard reaction was conducted under the following conditions: 473 K, 100 g of 10 wt.% propanol in water, 0.3 g catalyst.

2.4. Surface reactions studied by ATR-IR spectroscopy

A trapezoidal crystal of ZnSe (size 27.7 × 10 × 2 mm, angle of incidence of 60°) was coated with an aqueous suspension of the 3 wt.% Pt/γ-Al_2O_3 catalyst (50 mg catalyst and 500 mg deionized water prepared in an ultrasonic bath at 318 K, area 4 × 16 mm). The water in the suspension was evaporated at room temperature for 6 h and the thin catalyst film coated on the ATR crystal was reduced in hydrogen at 513 K at a rate of 1 K/min for 1 h. The thickness of the film was estimated to be 4 μm based on an alumina density of 3.27 g/cm^3. The ATR-IR spectra were recorded by using a stainless steel flow cell shown in Fig. 2 schematically. The ATR cell was placed in the IR spectrometer (Nicolet 5700 with a liquid nitrogen-cooled MCT detector) and the spectra were collected during reaction at a resolution of 4 cm^{-1} by accumulating 32 interferograms. After the reduction of the catalysts, a liquid glycerol solution (30 wt.%) was fed into the ATR cell with a HPLC pump at a rate of 0.01 ml/min. The pressure of the system was adjusted to 29 bar and the temperature was increased from room temperature to 498 K at a rate of 3 K/min.

3. Results

3.1. Catalysts characterization

The physicochemical properties of the Pt catalysts are summarized in Table 1. The concentration of Pt did not affect the specific surface area of the final catalyst, while the dispersion of the Pt particles decreased with the metal loading from 98% to 42%. The smallest average particle size of 1.1 nm was observed with the catalyst having the lowest Pt loading (1 wt.%). With increasing Pt loading (3 and 4.9 wt.%) the average diameter of the metal particles increased to 1.5 nm and 2.6 nm, respectively. The acid site concentration and base site concentration of the support were 0.15 and 0.05 mmol/g. It has to be noted, however, that these values serve only as an indication of the properties of the starting support, as the γ-Al_2O_3 has been converted to boehmite during the course of the reaction in water.

3.2. Influence of platinum particle size on catalytic properties

The overall catalytic conversion and the impact of the Pt particle size on the catalytic conversion of glycerol were studied at 498 K using a 20 wt.% glycerol solution and a total pressure of 29 bar (see Fig. 3). The main gaseous products formed were H_2 and CO_2 with small concentration of alkanes (C1–C3) and CO. The main oxygenated liquid products were 1,2-propanediol, hydroxyacetone, 1,2-ethanediol, and ethanol. All other products appear in much lower concentrations (see Tables 2 and 3).

While the rate of glycerol conversion increased only slightly with the metal particle size, the product distribution was more affected. The apparent selectivity to reforming (manifested by H_2 and CO_2) decreased with increasing metal particle size from 35% to 21%. CO was only formed in traces (400–1200 ppm), but it increased with the particle size in parallel to the formation of light alkanes. The formation rate of 1,2-propanediol (and to a lesser degree 1,2-ethanediol) also increased. The rate to ethanol was approximately constant, while the rate to hydroxyacetone de-

Table 1
Properties of the catalysts.

Pt loading (wt.%)	Surface area (m^2/g)	Average particle size (nm)	Dispersion (H/Pt)
0.98	104	1.1	0.98
2.97	105	1.5	0.75
4.88	102	2.6	0.42

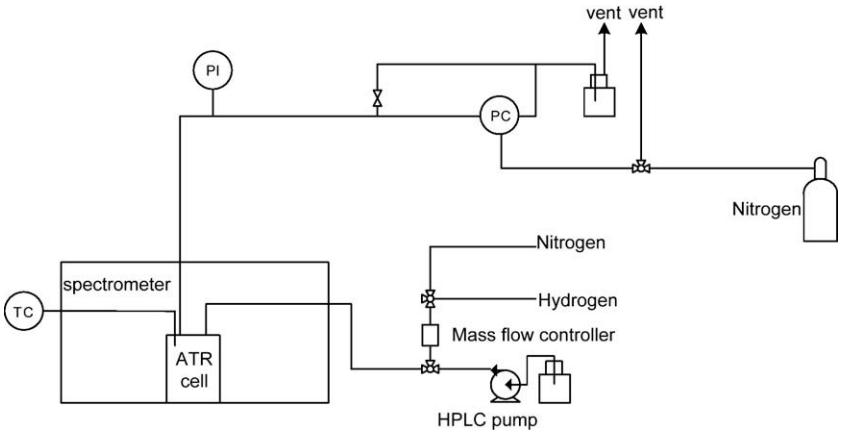

Fig. 2. Scheme of the reactor used for *in situ* ATR-IR spectroscopy.

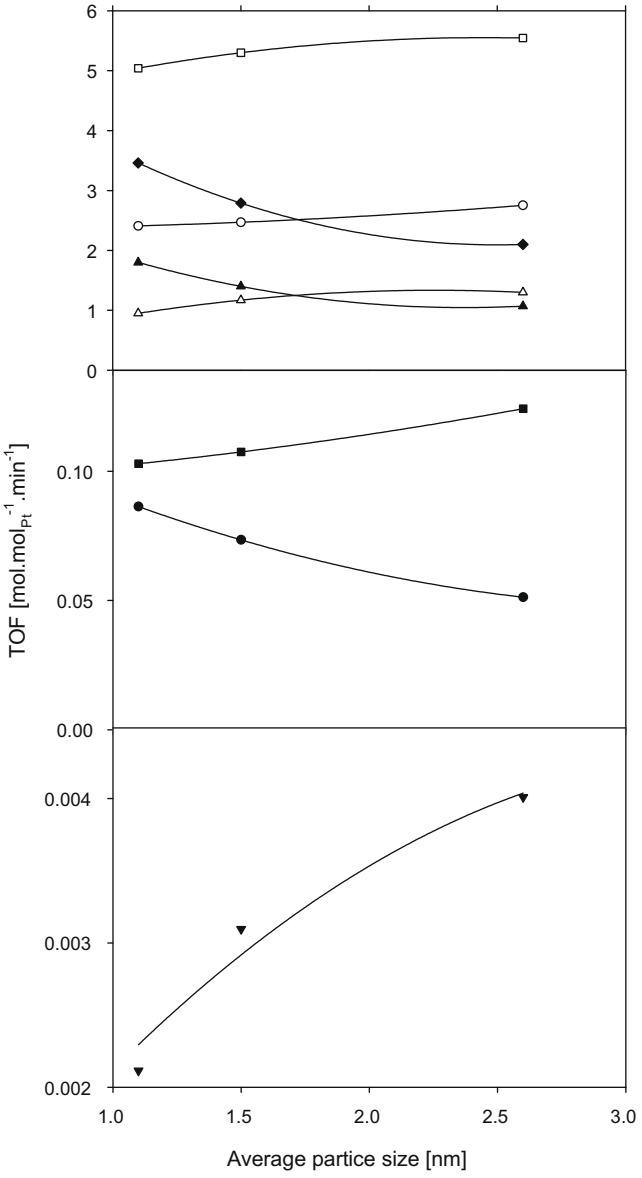

Fig. 3. TOF for the conversion of glycerol (□) and the formation of hydrogen (♦), carbon dioxide (▲), alkanes (■), carbon monoxide (▼), C1 oxygenated product (●), C2 oxygenated products (△), and C3 oxygenated products (○) (experimental conditions: T = 498 K, total pressure 29 bar, glycerol concentration 20 wt.%).

creased slightly. Thus, the most pronounced changes induced by increasing Pt particle size were the decrease of the formation of H_2 and CO_2 and the increase of hydrodeoxygenation. This change is in line with the decreasing concentration of metal sites, which favors the dehydration reactions.

3.3. Influence of glycerol concentration, total pressure, and conversion

The effect of glycerol concentration was studied with 3 wt.% Pt/Al_2O_3 at 498 K and 29 bar pressure. The TOF for glycerol and the formation of the main products are shown in Fig. 4. The rate increased for all products with the glycerol concentration. The apparent reaction order for the formation of liquid oxygenated products was approximately 0.8 and slightly lower (about 0.6) for the gaseous products (H_2, CO_2, CO, and alkanes).

The rates of glycerol conversion and of the formation of gaseous and liquid products as function of the total pressure over the 3 wt.% Pt/Al_2O_3 are shown in Fig. 5. The conversion of glycerol was not affected by the total pressure, the selectivity, however, changed drastically. The fraction of glycerol molecules that was converted to H_2 and CO_2 decreased from 43% at 26 bar to 12% at 45 bar. 1,2-Propanediol increased in parallel, while 1,2-propanol, 1,2-ethanediol and hydroxyacetone marginally increased.

The yields of the carbon containing main products and of H_2 as a function of the glycerol conversion are shown in Fig. 6. The highest yields were observed for the oxygenated products, which approached 45% at a glycerol conversion of 90%. The positive initial slope indicates that these are primary products. CO_2, the main carbon containing gaseous product of reforming and H_2 were formed with a similar yield at high conversion levels. With increasing conversion the slope steepens, which is an indication for the contribution of a secondary reaction pathway from intermediates. The yield for light alkanes increased only modestly with the conversion. The yields for the five main products 1,2-propanediol, ethanol, 1,2-ethanediol, 1-propanol, and 2-propanol are compiled in Fig. 7. Interestingly, ethanol increased markedly with increasing conversion indicating that it might be one of the most stable products in this process. For 1,2-propanediol and 1,2-ethanediol a maximum in the yield at around 50% conversion was observed.

3.4. Reactants and surface intermediates followed by ATR-IR spectroscopy

The ATR-IR spectra of the surface species during the reforming of glycerol in the aqueous phase on the Pt/Al_2O_3 catalyst at temperatures between 433 and 498 K and a pressure of 29 bar together with the spectra of hydroxyacetone and glyceraldehyde in an aque-

Table 2
Band assignments for oxygenated compounds.

Wavenumber (cm^{-1})			Bands assignment
Glycerol 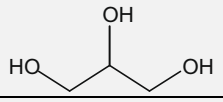	Glyceraldehyde 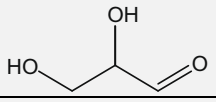	Hydroxyacetone 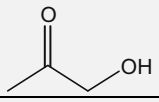	
–	1745	1720	C=O stretching
1390	1370	1417	COH deformation
1322	1300	1361	CH_2 twisting
1200	1254	1228	CH_2 twisting
1090	1142	–	C–O stretching (α-hydroxyl)
1035	1038	1085	C–O stretching (β-hydroxyl)
989	987	960	CH_2 rocking
975	979	–	CH_2 rocking

Table 3
Rates for the formation of gaseous products from glycerol and hydroxyacetone (experimental conditions: T = 498 K, total pressure 29 bar, catalysts 3 wt.% Pt/Al_2O_3).

Reactants	Gaseous products (rate based on carbon atom) (min^{-1})						Converted reactants (min^{-1})
	CO_2	C_2H_6	H_2	CH_4	CO	C_3H_8	
Glycerol (30 wt.%)	2.32	0.040	3.53	0.079	0.003	0.012	8.23
Hydroxyacetone (10 wt.%)	1.37	0.037	0.77	0.75	–	–	7.8

ous solution are shown in Fig. 8. The assignment of the characteristic bands to the reactant and intermediates is summarized in Table 2.

The bands at 1390, 1322, 1200, and 1090 cm^{-1} are assigned to the COH deformation vibration, to twisting and rocking vibrations of the CH_2 groups and to the stretching vibration of C–O at the α position in glycerol [25]. The bands above 1700 cm^{-1} indicate the presence of keto and aldehyde carbonyl groups. The band at 1640 cm^{-1} is assigned to the deformation vibration of OH groups in water.

Up to 433 K only water and glycerol were observed in the IR spectra measured under reaction conditions. Between 463 and 498 K, the temperature range used for the kinetic studies in the flow reactor, the band at 1720 cm^{-1} indicates the formation of keto or aldehyde carbonyl groups and the two broad bands at 2050 and 1940 cm^{-1} linear and bridged bonded CO on Pt [26,27]. In parallel to the detection of the adsorbed CO, two bands at 1510 and 1434 cm^{-1} were observed, which are attributed to the asymmetric and symmetric stretching vibrations of the surface carboxylates of ethanol and propanol on alumina [28].

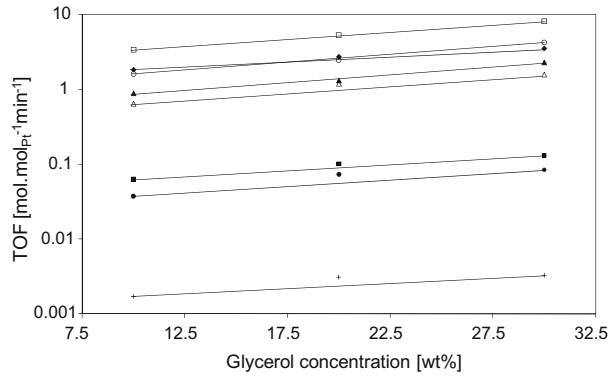

Fig. 4. TOF for the conversion of glycerol (□) and the formation hydrogen (♦), carbon dioxide (▲), alkanes (■), carbon monoxide (+), C1 oxygenated product (●), C2 oxygenated products (△), and C3 oxygenated products (○) on 3 wt.% Pt/Al_2O_3 (experimental conditions: T = 498 K, total pressure 29 bar).

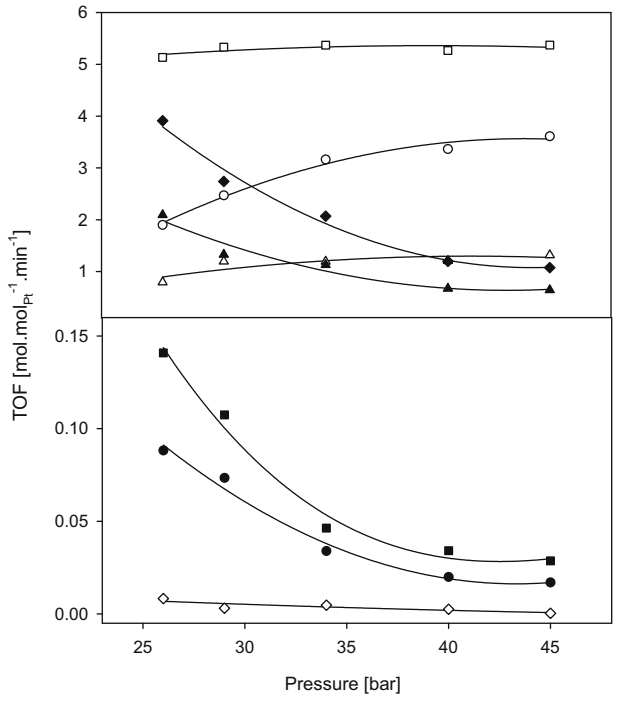

Fig. 5. Influence of total pressure on the TOF for the conversion of glycerol (□) and the formation of hydrogen (♦), carbon dioxide (▲), alkanes (■), carbon monoxide (◇), C1 oxygenated product (●), C2 oxygenated products (△), and C3 oxygenated products (○) on 38 wt.% Pt/Al_2O_3 (experimental conditions: T = 498 K, glycerol concentration 20 wt.%).

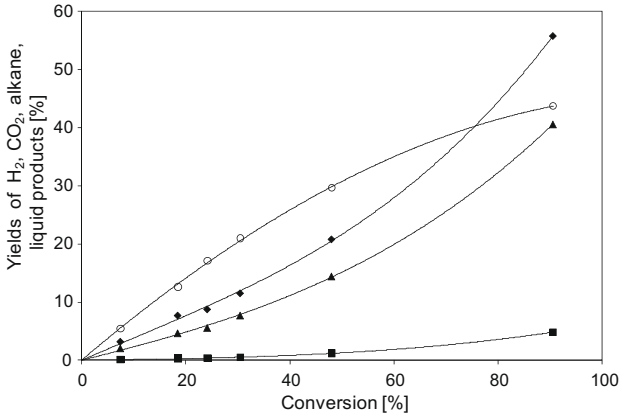

Fig. 6. Yields of H_2 (♦), carbon dioxide (▲), alkanes (■), and C1–C3 oxygenated products (○) as a function of conversion on 3 wt.% Pt/Al_2O_3 (experimental conditions: T = 498 K, total pressure 29 bar, glycerol concentration 30 wt.%).

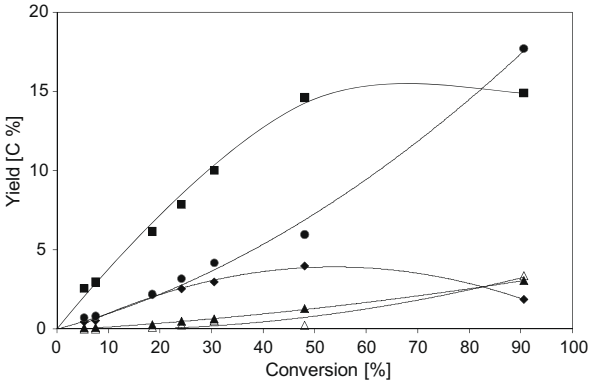

Fig. 7. Yields of carbon containing liquid products as a function of conversion; 1,2-propanediol (■), 1,2-ethanediol (♦), 2-propanol (△), 1-propanol (▲), and ethanol (●) on 3 wt.% Pt/Al_2O_3 (experimental conditions: T = 498 K, total pressure 29 bar, glycerol concentration 30 wt.%).

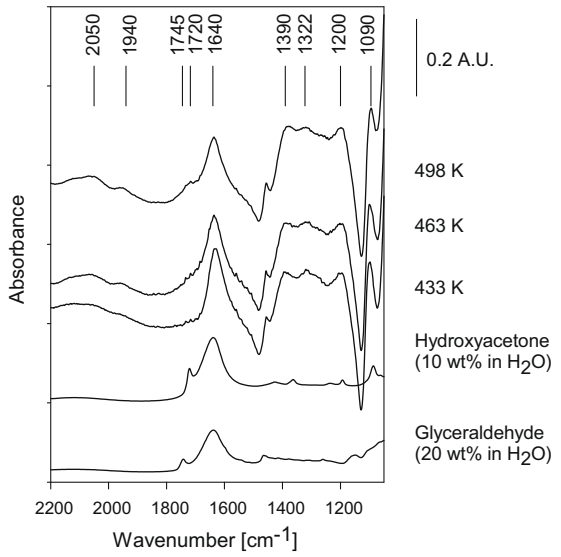

Fig. 8. ATR-IR spectra during reforming of 20 wt.% glycerol on 3 wt.% Pt/Al_2O_3, at 29 bar and 433, 463, and 498 K and of aqueous solutions of hydroxyacetone and glyceraldehyde.

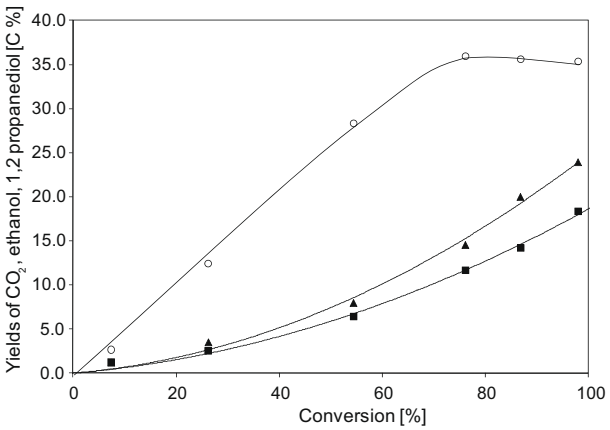

Fig. 9. Yields of carbon containing products as a function of hydroxyacetone conversion; carbon dioxide (▲), methanol (■), 1,2-propanediol (○) on 3 wt.% Pt/Al_2O_3 (experimental conditions: T = 498 K, total pressure 29 bar, hydroxyacetone concentration 10 wt.%).

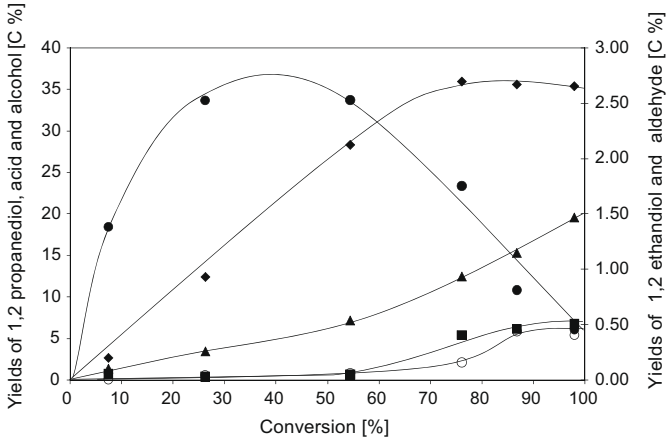

Fig. 10. Yields of carbon containing liquid products as a function of hydroxyacetone conversion; 1,2-propanediol (♦), aldehydes (acetaldehyde and propanal) (●), mono alcohols (methanol, ethanol, and propanol) (▲), 1,2-ethanediol (■), and acids (lactic acid, acetic acid, and propanoic acid) (○) on 3 wt.% Pt/Al_2O_3 (experimental conditions: T = 498 K, total pressure 29 bar, hydroxyacetone concentration 10 wt.%).

3.5. Reactions with liquid phase intermediate products

To explore surface species during the formation of the C3 oxygenated products, the conversion of hydroxyacetone, the most pronounced intermediate observed by ATR-IR spectroscopy, was studied. The rates for the formation of gaseous and liquid products are compiled in Tables 3 and 4, respectively. The main carbon containing gas phase products from hydroxyacetone conversion were CO_2 and methane. 1,2-Propanediol was the main product in the liquid phase. The yields of gas phase and liquid phase products for the conversion of hydroxyacetone are shown in Figs. 9 and 10. The C1–C3 oxygenated products were formed directly from hydroxyacetone, while alkanes, CO_2, and CO are the secondary products and must be formed via intermediate species. Among the oxygenated products, acetaldehyde and propanal were formed as primary, diols as the secondary products.

3.6. Reactions of 1-propanol and 2-propanol

The reactions with propanol were studied to understand the catalytic chemistry with the simplest alcohol having three carbon atoms. The results of 2-propanol and 1-propanol conversion are shown in Figs. 11 and 12, respectively. One notes that with 2-propanol acetone was the main reaction product, while the rate to dehydration was nearly two orders of magnitude slower. Neither hydrogen nor CO_2 was detected under the experimental conditions used. For 1-propanol propanal was the primary product, followed by ethane and CO_2 as well as propanoic acid. The overall level of decomposition suggests that the reaction starts with the dehydrogenation of 1-propanol followed by a surface reaction that allows the formation of the propionic acid (Cannizzaro reaction) or surface bound propylpropionate (Tishchenko reaction). Propanoic acid only appears in the reaction mixture after some delay indicating that either the catalyst has deactivated or a steady state at the surface has been achieved. The lower concentration of ethane compared to CO_2 is due to the type of sampling. Samples from the gas phase and the liquid phase were taken at regular intervals. However, the CO_2 dissolved in the aqueous phase cannot be accounted for as it will vent uncontrolled when the (cooled) liquid sample is expanded from reaction to atmospheric pressure. Control experiments with the pure alumina support showed at least two

Table 4
Rates for the formation of liquid products from glycerol and hydroxyacetone.

Reactant	Liquid products (rate based on carbon atom, min^{-1})												
	1	2	3	4	5	6	7	8	9	10	11	12	13
Glycerol (30 wt.%)	0.03	0.07	0.08	0.9	0.001	0.09	0.73	0.07	0.03	3.3	0.57	0.01	0.04
Hydroxyacetone (10 wt.%)	0.62	–	–	1.47	–	0.13	–	0.035	0.054	3.13	0.064	–	–

Liquid products: (1) acetaldehyde, (2) propanal, (3) methanol, (4) ethanol, (5) 2-propanol, (6) 1-propanol, (7) hydroxyacetone, (8) acetic acid, (9) propanoic acid, (10) 1,2-propanediol, (11) 1,2-ethanediol, (12) 1,3-propanediol, and (13) lactic acid.

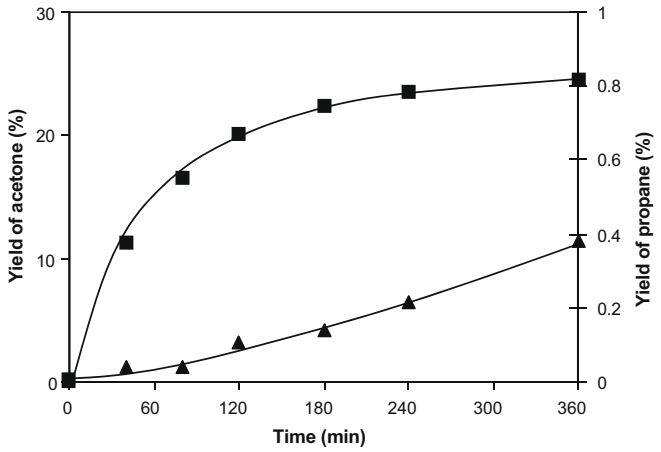

Fig. 11. Conversion of 2-propanol over 3 wt.% Pt/Al_2O_3 in the absence of hydrogen; propane (▲) and acetone (■) (experimental conditions: $T = 473$ K, total pressure 20 bar, 2-propanol concentration 10 wt.%).

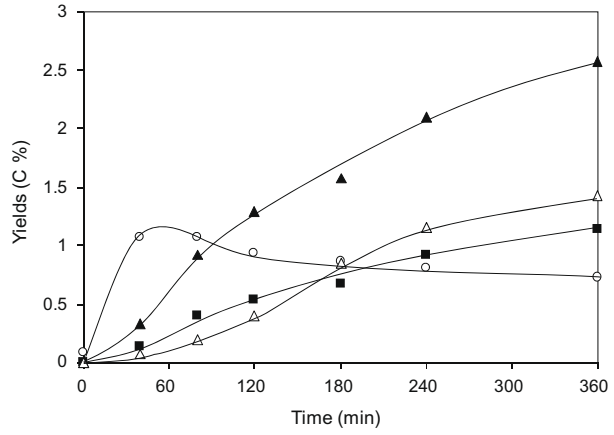

Fig. 12. Conversion of 1-propanol over 3 wt.% Pt/Al_2O_3 in the absence of hydrogen; ethane (▲), carbon dioxide (■), propanal (○), and propionic acid (△) (experimental conditions: $T = 473$ K, total pressure 20 bar, 1-propanol concentration 10 wt.%).

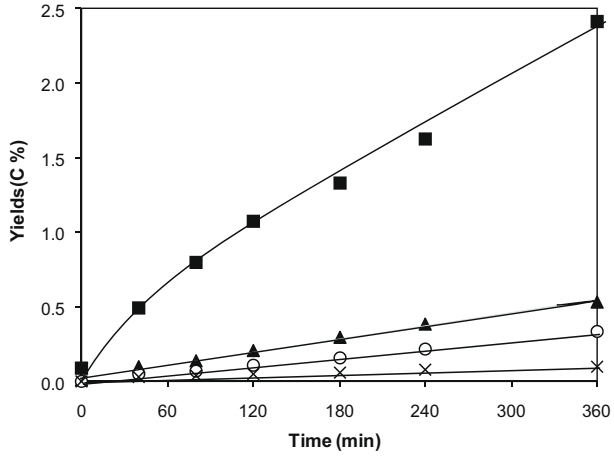

Fig. 13. Conversion of glycerol over Pt black in the absence of hydrogen; hydroxyacetone (■), carbon dioxide (▲), 1,2-propanediol (○), and ethylene glycol (×) (experimental conditions: $T = 473$ K, total pressure 16 bar, glycerol concentration 10 wt.%).

orders of magnitude slower conversion indicating that Pt is needed to catalyze the dehydrogenation.

3.7. Reactions of glycerol over unsupported Pt catalysts

Much of the chemistry described above has been ascribed also to reactions at the oxide support. As even weak metal support interactions may influence the behavior, we investigated also the conversion of glycerol over Pt black in the absence of hydrogen at a total pressure of 16 bar. The yields of the main products with time of reaction are shown in Fig. 13. The main product observed was hydroxyacetone. However, at a tenth of its rate also CO_2 was formed. 1,2-Propanediol (the hydrogenation product of hydroxyacetone) and ethylene glycol were also observed, which suggests that a small concentration of sites exists on Pt black able to rapidly catalyze the hydrogenation of the primary formed hydroxyacetone and dehydrogenation of glycerol to glyceraldehyde followed by disproportionation and decarboxylation or decarbonylation without appreciable concentrations of the intermediates being released into the liquid phase.

4. Discussion

The reactions occurring with glycerol in an aqueous phase with Pt/Al_2O_3 as a catalyst can be arranged into four main product groups, i.e., the conversion to hydrogen and CO_2, as well as products via glyceraldehyde, hydroxyacetone and 3-hydroxypropanal. We will show that the formation of hydrogen and CO_2 does not constitute a separate pathway, but follows from the transformation of the glycerol molecules in one dehydrogenation and two initial dehydration steps. The proposed reaction network is shown in Fig. 14. A large number of individual compounds were formed in very small concentrations and will not be discussed in detail. Only the most plausible routes for their formation are shown in the network.

Overall, we conclude that all routes require not only the presence of metal function, but also that of a Lewis acid–base component in order to catalyze the observed transformations. It will be shown, however, that unsupported Pt can assume under such conditions also the role of the solid acid. Because the conversion of 1-propanol and 2-propanol will allow explaining the principal chemistry of OH groups at the primary and secondary carbon atoms, their reactions will be discussed first. This should allow explaining the overall catalytic pathways with the more polar glycerol.

4.1. Conversion of 2-propanol and 1-propanol

Fig. 11 shows that the reaction of 2-propanol in water at 473 K led nearly exclusively to the dehydrogenation of propanol. The small amount of propane formed resulted presumably from the dehydration of the alcohol to propene on the support followed by the hydrogenation on the metal. As the presence of Pt is crucial to achieve high rates of 2-propanol dehydrogenation, we conclude that either the reaction takes place on the metal or that the metal facilitates the hydride abstraction in a more polar route. The fact that acetone is the only reaction product shows that the catalyst is not able to cleave C–C or C–O bond under the reaction conditions used. This is of high importance, as it establishes the absence of hydrogenolysis of the C–O bond in a secondary alcohol and also the inability to catalyze C–C bond hydrogenolysis.

In analogy, the conversion of 1-propanol led to the formation of propanal as the primary product. Ethane and CO_2 as well as propanoic acid were formed as the secondary products. Direct hydrogenolysis can be excluded as pathway to form ethane, as the C–C bond strengths in 1-propanol and 2-propanol differ by 50 kJ/mol (i.e., 357 kJ/mol of 1-propanol and 410 kJ/mol for 2-propanol [29]). The sequence suggests that once propanal is formed bimolecular surface reactions (Tishchenko/Cannizzaro type conver-

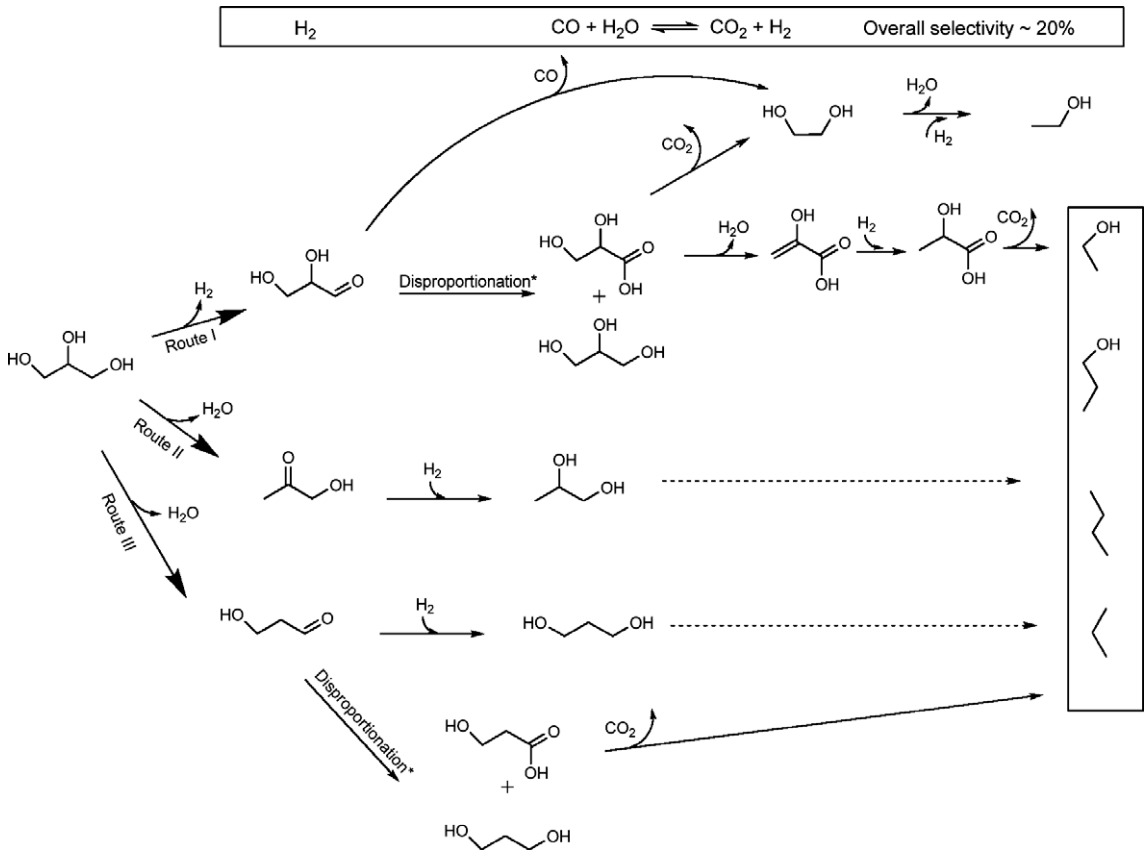

Fig. 14. Reaction pathways for an aqueous phase glycerol reforming, dotted arrows indicate a series of reactions in analogy to those depicted in route I (*either via Tishchenko or Cannizaro type reactions).

sions) lead to surface bound propanol and propanoic acid, which decarboxylates to ethane and CO_2 under the reaction conditions employed.

Of course, the parallel or exclusive decarbonylation cannot be excluded. Because the level of CO formed in this step is slightly higher (0.003 C%) than expected from the equilibrium value (0.0009 C%, given the observed CO_2 concentrations), we conclude that at least a fraction of the reactions leading to a carbon–carbon bond cleavage must result from decarbonylation. The fact that ethane and CO_2 are formed with a higher initial rate would point to decarbonylation followed by water gas shift reaction as the faster overall reaction pathway. A recent study using Ru catalysts suggests, however, that decarbonylation does not take place on molecular complexes in an aqueous phase using similar reaction conditions [30].

This is the first indication that the formation of hydrogen and CO_2 follows a pathway characterized by dehydrogenation, followed decarbonylation with a subsequent water gas shift reaction or disproportionation (Tishchenko or Cannizzaro type reactions) with a subsequent decarboxylation rather than by the more conventional metal-catalyzed routes of C–O and C–C bond splitting observed in hydrocarbon gas phase reforming.

At present the detailed mechanism for the disproportionation of the aldehyde into an acid and an alcohol cannot be differentiated. With respect to disproportionation, in the Tishchenko reaction (catalyzed by more acidic materials) formally the ester is formed, which will be hydrolyzed rapidly under the present reaction conditions. The Cannizzaro reaction, on the other hand, needs more basic catalysts. Both pathways are conceivable under the present conditions, as boehmite contains acid as well as basic sites acting as a weak anion exchanger [31].

Much like the differentiation of the disproportionation pathways, the unequivocal mechanistic differentiation between decarbonylation followed by water gas shift and disproportionation followed by decarboxylation of the acid is also very difficult. Propanoic acid is observed as an intermediate and decomposes to CO_2 and ethane (separate experiments, not shown). On the other hand, the rate of water gas shift is only twice of that of the alcohol conversion (glycerol), but shows nearly 0th order. This would be a sufficient boundary condition to explain the very low and nearly constant level of CO during the reaction of 1-propanol. Overall, we conclude, therefore, at present that both reactions occur in parallel.

4.2. Conversion of glycerol to hydrogen and CO_2

Deductions on the mechanism of the formation of H_2 and CO_2 are only inferred indirectly at present assuming that the mechanistic aspects of the fundamental reactions are the same for glycerol as for propanol.

The overall reaction is concluded to be catalyzed by Pt because of the sympathetic variation of the rate of reaction with the concentration of the available Pt. The results show that hydrogen is generated by the dehydrogenation of hydroxy groups at primary carbon atoms and carbon oxides are formed subsequent to this dehydrogenation via decarbonylation (additional hydrogen is formed by rapid water gas shift) or disproportionation of two aldehydes followed by decarboxylation. The most effective route to hydrogen and carbon oxides proceeds via glyceraldehyde as a primary product. In general, aldehydic and carboxylic groups are the precursors of carbon oxide formation. The similarities in bond energies in glycerol and the alcohols let us to exclude other hydrogenolytic steps for cleaving C–O or C=C bond [29].

It should be mentioned that under the present experimental conditions the level of CO has been found to be slightly, but constantly, above the partial pressure expected from the water gas shift equilibrium. This indicates that at least a part of the CO_2 has been generated by decarbonylation followed by water gas shift. Unfortunately, at present the relative importance of the two reaction pathways of decarbonylation and decarboxylation can only be estimated as isotope labeling experiments would not lead to unequivocal conclusions, i.e., both reaction pathways produce oxygen isotope scrambling in CO_2. It is remarkable, however, that under no circumstances a kinetic pathway of CO_2 as the secondary product from CO has been observed, although the rate of glycerol conversion and of water gas shift differ only by a factor of two.

The rate of hydrogen evolution is somewhat lower than expected on the basis of the rate of CO_2 formation (i.e., $H_2/CO_2 = 1.9$ vs. 2.3 for the stoichiometry of the reforming reaction). This difference is attributed to a fraction of hydrogen being used for the hydrogenation of unsaturated intermediates.

With increasing particle size CO_2 and H_2 formation decreased in parallel, while the rates to oxygenated C2 and C3 products from hydrodeoxygenation increased. A closer analysis shows that the H_2 and CO_2 formation decrease by a factor of 1.6, as approximately the same fraction of hydrogen is used for the hydrogenation of unsaturated products formed along the other reaction pathways. This indicates that the ability for dehydrogenation, decarbonylation/water gas shift as well as disproportionation and decarboxylation are disfavored by a critical factor of the larger particle size, i.e., by the lower concentration of highly coordinatively unsaturated metal atoms and/or by a lower concentration of metal atoms at the support-metal boundary.

Increasing the total pressure has surprisingly a similar effect than increasing the Pt particle size. At a constant glycerol conversion (see Fig. 5) the rate of H_2 and CO_2 evolution decreased by factors of 3.7 and 3.2, respectively, which has kinetic reasons. The differences between H_2 and CO_2 indicates that relatively more H_2 is used to hydrogenate reaction intermediates, i.e., to form the alcohols, in particular 1,2-propanediol, as the hydrogen and CO_2 formation is retarded. From the increase in the selectivity to CO_2 and the hydrodeoxygenated products in parallel with increasing conversion, we estimate that about 20% of the hydrogen produced is used in the hydrogenation of products from dehydration. We conclude that this is primarily related to the higher rate of hydrogenation of aldehydic and ketonic intermediates, e.g., hydroxyacetone, which form via dehydration on the boehmite support. The higher hydrogen pressure shifts the equilibrium between the glycerol and the aldehyde intermediates, thus, preventing the subsequent decarbonylation or disproportionation reactions to acids and alcohols, which lead eventually decarboxylation.

The alkanes formed in small concentrations appear to result primarily from the decarbonylation or decarboxylation of intermediates that have undergone dehydration before. It is interesting to note that this reaction route decreases markedly in importance with increasing the overall pressure.

The three primary carbon containing reaction products are formed by dehydrogenation (glyceraldehyde) and dehydration of the hydroxy group at the secondary and primary carbon atom (hydroxyacetone and 1-hydroxypropionaldehyde). It is important to note that acid–base catalyzed dehydration (which also takes place on Pt black) is the first step in two of the three reaction pathways. Dehydration is only possible with glycerol, but not with propanol, which is attributed to the higher polarity in glycerol compared to the mono- and di-alcohols [32]. Molecules with keto and aldehydic groups have also been observed by *in situ-IR* spectroscopy (see Fig. 8) indicating their presence as intermediates at least on the catalyst support.

4.3. Formation of products via glyceraldehyde (reaction route I)

In this reaction pathway glycerol is concluded to be dehydrogenated to glyceraldehyde on Pt, which is rapidly decarbonylated or converted via a Tishchenko/Cannizzarro type disproportionation to glyceric acid and to glycerol over acid–base sites of boehmite (the transformed alumina support) [33,34]. The rate of these reactions combined appears to be so fast that glyceraldehyde is not found in the liquid phase. As it has been shown for propanol, the cleavage of C–C bond of alcohols in the liquid phase under the presently used reaction conditions it is highly unlikely to occur via a hydrogenolytic pathway. Therefore, 1,2-ethanediol and ethanol are concluded to be formed either via decarbonylation of glyceraldehyde or via decarboxylation of glyceric acid. Ethanediol is subsequently dehydrated to acetaldehyde that in turn is hydrogenated to ethanol. An alternative route for the conversion of glyceric acid is the dehydration to 2-2-hydroxyprop-2-enoic acid (hydroxy acrylic acid), which in turn is hydrogenated to lactic acid. As the concentration of lactic acid in the product is at least one order of magnitude lower than that of 1,2-ethanediol and ethanol the latter reaction appears to play only a minor role.

The additional formation of CO_2 and H_2, observed at higher conversion levels (see Fig. 6) as a secondary reaction is attributed to additional reactions of ethanediol via dehydrogenation, disproportionation and further decarbonylation and decarboxylation reactions. It should be noted that the reactivity of the intermediately formed aldehydes and acids for decarbonylation and decarboxylation decreases with decreasing degree of hydroxylation.

4.4. Formation of products via hydroxyacetone (route II)

2-Hydroxyacetone formed by the dehydration of glycerol dominates as a primary product for the liquid phase reaction at all pressures and can be made with rather high selectivity, if the pressure is further increased [35]. The absence of 1,2-propendiol indicates that the enol–keto transformation takes place on the catalyst surface without desorption after the initial cleavage of one hydroxyl group. It is important to note that ketones have been observed in the adsorbed state during *in situ* ATR-IR spectroscopic experiments. However, the actual concentrations of these molecules in the liquid phase products are low under all conditions. A H_2/CO_2 ratio of 0.55 was observed for the reforming of hydroxyacetone (see Table 2), which is significantly lower than stoichiometric ratio expected from the classic combination of reforming and water gas shift reactions ($H_2/CO_2 = 2.33$). This can be explained by the fact that methane is formed in stoichiometric amounts so that two CO_2 molecules and only one H_2 molecule are produced.

The present results are in agreement with earlier results of glycerol "hydrogenolysis" over the metal group VIII supported catalyst [36–38], which also described hydroxyacetone as the major intermediate for 1,2-propanediol formation, while the bimolecular dehydration leading to $C_6H_{14}O_5$ mentioned in Ref. [20] was not observed. At high conversion levels the yield of 1,2-propanediol decreases, while the yields to mono alcohols, H_2, and carbon dioxide increased sharply, which indicates that 1,2-propanediol undergoes further reactions via analogous reaction pathways as described above.

4.5. Formation of products via 3-hydroxypropanal (route III)

Like with reaction route II dehydration of glycerol to 3-hydroxypropanal is catalyzed on the acid sites. As 3-hydroxypropanal is more reactive compared to hydroxyacetone it was not observed as an intermediate in the liquid phase. Three reaction routes are feasible, i.e., hydrogenation to 1,3-propanediol, decarbonylation and a Tishchenko/Cannizzaro type disproportionation to 1,3-pro-

panediol and 3-hydroxypropanoic acid, which can subsequently react to ethanol via decarboxylation. As only minor concentrations of 1,3-propanediol were formed compared to 1,2-propanediol, this route contributes to a much lesser extent to the formation of products compared to routes I and II.

5. Conclusions

Using the catalytic conversion of 1-propanol and 2-propanol, it has been shown that under the conditions typically used for an aqueous phase reforming, hydrogenolysis of C–C and C–O bonds does not take place. Instead it is concluded that the catalytic reactions of alcohols in the aqueous phase occur as bifunctional reactions over catalysts involving metal and support acid–base functions. Dehydrogenation and dehydration reactions are seen as the dominating initial steps. Note that Pt black seems to be able to act as a solid acid catalyzing dehydration. It is remarkable that with Pt black the rate of dehydration is faster than the rate of dehydrogenation (seen only through the subsequent products of decarbonylation/water gas shift or disproportionation decarboxylation).

Decarbonylation and Tishchenko/Cannizaro type disproportionation reactions (of course also crossed Cannizzaro reactions) followed by decarboxylation of the acid follow the dehydrogenation and dehydration in the first step. The results show unequivocally that not only the liquid phase products, but also CO_2, CO, and H_2 are formed via this reaction sequence. In turn, the formation of alkanes is caused primarily by the elimination of water and the rapid hydrogenation of olefins. Non-oxofunctionalized carbon in molecules cannot be converted to hydrogen and carbon oxides and will appear as alkanes in the products.

A reaction network consisting of three parallel routes can be constructed that includes dehydrogenation and dehydration of glycerol as well as the products expected by typical reforming. Using the indirect evidence of propanol reactions in aqueous phase, we conclude that "aqueous phase reforming" proceeds via the dehydrogenation of glycerol to glyceraldehyde or the analogous dehydrogenation of hydroxyl groups at the primary carbon atoms. As long as water is not eliminated, a shorter alcohol is produced in each decarbonylation or disproportionation/decarboxylation step, which then undergoes again the same reaction sequence leading finally in the expected mixture of H_2 and CO_2.

The ratio between H_2 and CO_2 formed indicates that about 20% of the hydrogen produced reacts further in the liquid phase. A fraction of the molecules that form dihydroxy propanoic acid from glyceraldehyde is transformed to 1,2-ethanediol, which is partially converted by dehydration and hydrogenation to ethanol. Lactic acid is formed via the dehydration of dihydroxy propanoic acid and subsequent hydrogenation. Overall, mono alcohols and alkanes are formed in the secondary bifunctional reactions via acid-catalyzed dehydration and decarbonylation or decarboxylation reactions as well as metal-catalyzed hydrogenation reactions.

Two reaction pathways of glycerol are based on dehydration (routes II and III) in the first step. As carbon atoms are formed in these steps that do not have a C–O bond directly attached a higher fraction of hydrocarbons and alcohols is produced via these pathways.

In general, for all reaction pathways in the liquid phase higher partial pressure of hydrogen (higher total pressure in this study) disfavors the presence of aldehydes and consequently limits the reactions leading to CO_2 formation. This in turn favors all reactions that can be catalyzed by oxidized parts of the metal or by the support (e.g., dehydration). Similarly a larger particle size limits the relative availability of the metal function and, therefore, favors the catalytic chemistry induced by the support.

The present study shows that the results of conversions of alcohols and polyalcohols can be explained by bifunctional reactions involving support and metal phase. The unusual behavior of Pt black indicates, however, that Pt may act as both as acidic solid via surface hydroxyl groups and as metal able to (de)hydrogenate and catalyze decarbonylation and decarboxylation.

Acknowledgments

This work was supported by the European Union in the framework of the Integrated Project TOPCOMBI (NMP2-CT-2005-515792-2). The authors are further grateful to the fruitful discussions with Prof. G. Fuentes and within the European network of excellence IDECAT.

References

[1] G.W. Huber, S. Iborra, A. Corma, Chem. Rev. 106 (2006) 4044.
[2] S. Czernik, R. French, C. Feik, E. Chornet, Ind. Eng. Chem. Res. 41 (2002) 4209.
[3] T. Hirai, N. Ikenaga, T. Miyake, T. Suzuki, Energy Fuels 19 (2005) 1761.
[4] B. Zhang, X. Tang, Y. Li, Y. Xu, W. Shen, J. Hydrogen Energy 32 (2007) 2367.
[5] S. Adhikari, S. Fernando, S.D. Filio, M. Bricka, P.H. Steele, A. Haryanto, Energy Fuels 22 (2008) 1220.
[6] G.W. Huber, A. Corma, Angew. Chem. Int. Ed. 46 (2007) 7184.
[7] R.D. Cortright, R.R. Davda, J.A. Dumesic, Nature 418 (2002) 964.
[8] J.W. Shabaker, G.W. Huber, J.A. Dumesic, J. Catal. 222 (2004) 180.
[9] G.W. Huber, J.W. Shabaker, J.A. Dumesic, Science 300 (2003) 2075.
[10] G.W. Huber, J.A. Dumesic, Catal. Today 111 (2006) 119.
[11] J.W. Huber, J.W. Shabaker, S.T. Evans, J.A. Dumesic, Appl. Catal. B: Environ. 62 (2006) 226.
[12] J.W. Shabaker, D.A. Simonetti, R.D. Cortright, J.A. Dumesic, J. Catal. 231 (2005) 67.
[13] J.W. Shabaker, R.R. Davda, G.W. Huber, R.D. Cortright, J.A. Dumesic, J. Catal. 215 (2003) 344.
[14] J.W. Shabacker, J.A. Dumesic, Ind. Eng. Chem. Res. 43 (2004) 3105.
[15] X. Wang, S. Li, H. Wang, B. Liu, X. Ma, Energy Fuels 22 (2008) 4285.
[16] E.P. Maris, R.J. Davis, J. Catal. 249 (2007) 328.
[17] E.P. Maris, W.C. Ketchie, M. Murayama, R.J. Davis, J. Catal. 251 (2007) 281.
[18] R.R. Davda, J.W. Shabaker, G.W. Huber, R.D. Cortright, J.A. Dumesic, Appl. Catal. B: Environ. 43 (2003) 13.
[19] J.W. Shabaker, G.W. Huber, R.R. Davda, R.D. Cortright, J.A. Dumesic, Catal. Lett. 88 (2003) 1.
[20] N. Luo, X. Fu, F. Cao, T. Xiao, P.P. Edwards, Fuel 87 (2008) 3483.
[21] K. Lehnert, P. Claus, Catal. Commun. 9 (2008) 2543.
[22] C. Zhao, Y. Kou, A.A. Lemonidou, X. Li, J.A. Lercher, Angew. Chem. Int. Ed. 48 (2009) 3987.
[23] P.H. Lewis, J. Catal. 11 (1968) 162.
[24] G. Vergeret, P. Gallezot, in: G. Ertl, H. Knözinger, J. Weitkamp (Eds.), Handbook of Heterogeneous Catalysis, vol. 2, Wiley-VCH, Weinheim, 1997, p. 439.
[25] D. Lin-Vien, N.B. Colthup, W.G. Fateley, G. Grasselli, Infrared and Raman Characteristic Frequencies of Organic Molecules, Academic Press, San Diego, 1991.
[26] B.E. Hayden, A.M. Bradshaw, Surf. Sci. 125 (1983) 787.
[27] F. Kitamura, M. Takede, M. Takahashi, M. Ito, Chem. Phys. Lett. 142 (1987) 318.
[28] J. Cunningham, B.K. Hodnett, M. Illyas, J. Tobin, E.L. Leahy, J.L.G. Fierro, J. Chem. Soc. Faraday Discuss. 72 (1981) 283.
[29] Y.R. Luo, in: Comprehensive Handbook of Chemical Bond Energies, CRC Press, Boca Raton, Florida, 2007, p. 178.
[30] D. Taher, M.E. Thibault, D. Di Mondo, M. Jennings, M. Schlaf, Chem. Eur. J. 15 (2009) 10132.
[31] P. Raybaud, M. Digne, R. Iftimie, W. Wellens, P. Euzen, H. Toulhoat, J. Catal. 201 (2001) 236.
[32] E.P. Hunter, S.G. Lias, J. Phys. Chem. Ref. Data 27 (1998) 413.
[33] C. Keresszegi, D. Ferri, T. Mallat, A. Baiker, J. Phys. Chem. B 109 (2005) 958.
[34] A.E.T. Kuiper, J. Medema, J.J.G.M. Bokhoven, J. Catal. 29 (1973) 40.
[35] E. D'Hondt, S.V. de Vyver, B.F. Sels, P.A. Jacobs, Chem. Commun. (2008) 6011.
[36] M.C. Ramos, A.I. Navascues, L. Garcia, R. Bilbao, Ind. Eng. Chem. Res. 46 (2007) 2399.
[37] M.A. Dasari, P. Kiatsimkul, W.R. Sutterlin, G.J. Suppes, Appl. Catal. A: Gen. 281 (2005) 225.
[38] S. Wang, H. Liu, Catal. Lett. 117 (2007) 1.